RM L55D29

NACA

RESEARCH MEMORANDUM

INVESTIGATION OF THE EFFECTS OF MODEL SCALE AND STREAM REYNOLDS NUMBER ON THE AERODYNAMIC CHARACTERISTICS OF TWO RECTANGULAR WINGS AT SUPERSONIC SPEEDS IN THE LANGLEY 9-INCH SUPERSONIC TUNNEL

By Donald E. Coletti

Langley Aeronautical Laboratory
Langley Field, Va.

NATIONAL ADVISORY COMMITTEE FOR AERONAUTICS

WASHINGTON

June 14, 1955
Declassified April 8, 1957

NATIONAL ADVISORY COMMITTEE FOR AERONAUTICS

RESEARCH MEMORANDUM

INVESTIGATION OF THE EFFECTS OF MODEL SCALE AND STREAM REYNOLDS NUMBER ON THE AERODYNAMIC CHARACTERISTICS OF TWO RECTANGULAR WINGS AT SUPERSONIC SPEEDS IN THE LANGLEY 9-INCH SUPERSONIC TUNNEL

By Donald E. Coletti

SUMMARY

An investigation has been made in the Langley 9-inch supersonic tunnel at Mach numbers 1.62, 1.94, and 2.41 to determine the effects of model scale and stream Reynolds number on the lift, drag, and pitching moment of two geometrically similar rectangular wings. The wings had symmetrical circular-arc cross sections with aspect ratios of 1.80, thickness ratios of 0.059, and a scale factor of approximately 0.52. The Reynolds numbers of the tests based on the wing chords varied between 0.13×10^6 and 2.96×10^6.

The results show that effects of scale are small and, in most cases, negligible. With minor exceptions at the very low Reynolds numbers of these tests, the effect of increasing Reynolds number (by increasing tunnel stagnation pressure) was to increase the lift, decrease the pitching moment, and decrease the drag in a manner consistent with the change in laminar skin-friction drag to a point where transition appeared to occur.

INTRODUCTION

The present availability of experimental information on the effects of model scale and of stream Reynolds number of the flow on the aerodynamic characteristics of a rectangular wing is somewhat meager and isolated. Some results due to scale and Reynolds number effects may be found in references 1 to 6. References 1 to 5 contain information obtained at subsonic speeds for wings alone, and reference 6 contains results for wing-body combinations obtained at both subsonic and supersonic speeds.

The purpose of the present investigation was to make a series of tests in the Langley 9-inch supersonic tunnel to determine the effect of model scale for a range of Reynolds numbers by observing the variations in lift-curve and pitching-moment-curve slopes and minimum drag coefficients of two geometrically similar rectangular wings. A secondary purpose of the test program was to determine the effect of a stream Reynolds number variation on the aerodynamic characteristics of the same two rectangular wings. The wings had symmetrical circular-arc cross sections with aspect ratios of 1.80, thickness ratios of 0.059, and a scale factor of approximately 0.52. The tests were conducted at Reynolds numbers varying between 0.13×10^6 and 2.96×10^6 (based on the wing chords) and at Mach numbers of 1.62, 1.94, and 2.41. The angle of attack of the wings was varied between 7° and -6°.

SYMBOLS

A	aspect ratio, $\frac{b}{c}$
b	wing span
c	wing chord
α	angle of attack
C_L	lift coefficient, $\frac{\text{Lift}}{qS}$
C_m	pitching-moment coefficient about 50 percent chord, $\frac{\text{Moment}}{qSc}$
C_D	drag coefficient, $\frac{\text{Drag}}{qS}$
$C_{L_\alpha} = \frac{dC_L}{d\alpha}$ at $C_L = 0$	
$C_{m_\alpha} = \frac{dC_m}{d\alpha}$ at $C_L = 0$	
C_{D_W}	theoretical wave-drag coefficient

C_{D_f}(lam.)	theoretical laminar skin-friction drag coefficient
C_{D_f}(turb.)	theoretical turbulent skin-friction drag coefficient
c.p.	center of pressure
M	Mach number
q	dynamic pressure, $\frac{\rho V^2}{2}$
ρ	stream density
R	Reynolds number, $\frac{\rho V c}{\mu}$
S	wing area
t	maximum wing thickness
t/c	thickness ratio
V	free-stream velocity
μ	coefficient of viscosity

APPARATUS AND TESTS

Tunnel

The Langley 9-inch supersonic tunnel is a closed-throat, single return, continuous operating tunnel in which the test section is approximately 9 inches square. Different test Mach numbers are achieved through the use of interchangeable nozzle blocks. Eleven fine-mesh turbulence-damping screens are installed in the settling chamber ahead of the supersonic nozzle. The pressure, temperature, and humidity can be controlled during the tunnel operation.

Models

The models consisted of two geometrically similar rectangular wings, each having a symmetrical circular-arc cross section and an aspect ratio of 1.80 and a thickness ratio of 0.059. The size of one wing along with

the sting and windshield was reduced by a scale factor of approximately 0.52 from that of a larger wing. A sketch of the large wing with the pertinent dimensions is shown in figure 1.

Balances

The lifts, drags, and pitching moments of the two wings were obtained on two external balances of the Langley 9-inch supersonic tunnel. Some of the tests were made with an earlier balance (mentioned herein as the old balance) whereas the remaining tests were made with a later balance (hereafter referred to as the new balance). The old balance contained a system of self-balancing beam scales capable of measuring three components, lift, drag, and pitching moment, at stagnation pressures of the order of 1 atmosphere. After the repowering of the tunnel (to extend the Reynolds number range), the old balance was modified to convert it into a six-component balance capable of measuring forces at stagnation pressures of the order of 4 atmospheres. The sting mounting of the wings was identical for both balances, the rear portion of the sting being enclosed by a windshield so that all unnecessary external forces could be eliminated. As seen in figure 1, the nose of the windshield was made flush with the sting shoulder and the pressure within was adjusted to free-stream static pressure.

Corrections, which have been standardized and considered routine for wing-sting tests in this facility, were applied to the drag of the wing-sting configurations to account for the difference between free-stream pressure and the pressure at the base of the support sting shoulder.

Tests

Tests were conducted at Mach numbers of 1.62, 1.94, and 2.41. Measurements were made of the lift, drag, and pitching moment about the 50 percent chord. Reynolds numbers of the tests based on the wing chords were varied between 0.13×10^6 and 2.73×10^6 at $M = 1.62$, between 0.13×10^6 and 2.96×10^6 at $M = 1.94$, and between 0.19×10^6 and 2.59×10^6 at $M = 2.41$. The Reynolds number for each wing was varied by changing the tunnel stagnation pressure. The angle of attack of each wing was indicated on a scale, graduated in degrees, by means of a light beam reflected from a small mirror mounted flush on the sting as shown in figure 1. The range of angle of attack was between 7° and -6°. Throughout the tests the dewpoint in the tunnel was maintained at a level where condensation effects would be negligible.

PRECISION OF DATA

The probable accuracies of the test variables and aerodynamic quantities at all Mach numbers and at Reynolds numbers of 0.20×10^6 and 2.8×10^6 are believed to be within the limits given in the following table:

R	C_{L_α}	C_{m_α}	Center of pressure, percent	$C_{D_{min}}$	R	M	α, deg	
							Average initial	Relative
0.20×10^6 2.80×10^6	±0.0005 ± .0001	±0.0007 ± .0001	±2.11 ± .24	±0.0009 ± .0001	±25,000 ±12,000	±0.01 ± .01	±0.14 ± .14	±0.01 ± .01

PRESENTATION OF DATA

The aerodynamic quantities of the large rectangular wing obtained on the old and the new balances are presented in figures 2, 3, and 4 at Mach numbers 1.62, 1.94, and 2.41, respectively. The aerodynamic quantities of the small rectangular wing also obtained on the old and new balances are shown in figures 5, 6, and 7 at Mach numbers 1.62, 1.94, and 2.41, respectively. The various Reynolds numbers at which all of the data were obtained are given in these figures.

It will be noted in figures 3(a), 3(b), and 3(c) at $R = 2.96 \times 10^6$ (large wing) and figures 5(a), 5(b), and 5(c) at $R = 1.54 \times 10^6$ (small wing) that the range of angle of attack is somewhat limited. This was due to the wings failing structurally because of high loads incurred as a result of unfortunate failure of electrical power to the tunnel drive system.

Some of the lift data obtained on the old balance at large negative angles of attack ($\alpha < -2^\circ$) has been omitted (see, for example, figs. 4(a) and 4(b)) to facilitate presentation of the data.

The variation of lift-curve slopes, pitching-moment-curve slopes, centers of pressure, and minimum drag coefficients for the two wings with a variation of Reynolds number is given in figures 8 and 9 for each of the three Mach numbers investigated. Comparison between the experimental results and theory is also given in the two figures.

RESULTS AND DISCUSSION

Lift

It is seen from figure 8 that good agreement is obtained between the large and small wings with the exception at Mach numbers 1.62 and 1.94 between $R = 0.9 \times 10^6$ and 1.6×10^6. For these Mach numbers and Reynolds numbers, the lift-curve slopes of the small wing are greater than those of the large wing. The difference in lift-curve slopes between the two wings is believed to be due to a variation of the turbulence level with stagnation pressure in the tunnel. It has been shown in reference 7 that the turbulence level in the entrance cone of the Langley 9-inch supersonic tunnel increases with increasing stagnation pressure. If the turbulence level in the test section also increases with increasing stagnation pressure, it is possible that at the highest Reynolds number (or highest stagnation pressure), the level of turbulence may be sufficient to create a turbulent boundary layer on the small wing and thereby reduce any separation that existed on the small wing. Under such conditions the lift of the small wing would be greater than the lift of the large wing at the same Reynolds number (but at a reduced stagnation pressure).

On the basis of the above reasoning, one might logically conclude that the transition Reynolds number will decrease with increasing stagnation pressure. However, numerous experimental results are available that oppose this conclusion. Results of experiments with a variety of model configurations at several Mach numbers and in several tunnels (see ref. 8) show that transition Reynolds number increases with increasing tunnel stagnation pressure. At the present time, no satisfactory explanation has been found for this phenomena. Therefore in view of the contradictory conclusions between the experimental results and the logical expectations, it would be very difficult to attribute the lift differences between the small and large wings to a simple scale effect, that is, changes in model dimensions.

As shown in figure 8, an increase in Reynolds number (by increasing stagnation pressure) causes an increase in lift-curve slope for both the large and small wings. However, the rate of increase of lift-curve slope with Reynolds number generally decreases with increasing Mach number. The lift-curve slope at $M = 1.62$ increases as much as 18 percent over the Reynolds number range whereas at $M = 2.41$ the increase is only 10 percent.

Theoretical values of lift-curve slope obtained from reference 9 are also presented in figure 8. At Mach numbers of 1.62 and 1.94, the predicted values agree with the experimental values at the intermediate

Reynolds numbers, but at the high Reynolds numbers experiment is underpredicted and at the low Reynolds numbers it is overpredicted. At a Mach number of 2.41, the agreement between experiment and theory is very good throughout the Reynolds number range.

Pitching Moment

The pitching-moment-curve slopes of figure 8 are presented using a large ordinate scale so that effects due to the Mach number and Reynolds number might be more readily observed and compared. In view of the overall accuracy of the measurements (± 0.0007 at $R = 0.20 \times 10^6$ and ± 0.0001 at $R = 2.80 \times 10^6$) it is probable that the differences in the pitching-moment-curve slopes of the two wings at each Mach number are not too significant and, as a result, would seem to indicate no effect due to model scale.

It is further seen that the pitching-moment-curve slopes of the two wings increase to a maximum value at the very low Reynolds numbers and then decrease at a decreasing rate as the Reynolds number is further increased. This occurs at all the Mach numbers investigated. The pitching-moment-curve slope at $M = 1.62$ varies approximately 23 percent over the Reynolds number range whereas at $M = 2.41$ the variation is as much as 34 percent.

Theoretical values of pitching-moment-curve slope obtained from reference 9 are in poor agreement with the experimental results at all the Mach numbers and Reynolds numbers of this investigation.

Center of Pressure

The theoretical locations of center of pressure shown in figure 8 are between 5 and 10 percent rearward of the experimental locations. In general, there appears to be no significant effect due to scale throughout the Reynolds number range.

Even though the quantitative agreement between theory and experiment is not too favorable for the center-of-pressure locations, there is agreement qualitatively in the effect of Mach number. At any Mach number of this investigation the location of the center of pressure moves toward the leading edge at the low Reynolds numbers and then gradually shifts rearward at a decreasing rate with increasing Reynolds number to a constant location at the higher Reynolds numbers.

Drag

It is seen in figure 9 that there are little or no significant differences in the minimum drag coefficients between the large and small wings at the three Mach numbers and over the Reynolds number range with the exception at Mach number 1.62 and above a Reynolds number of 1.2×10^6. At this Mach number and above this Reynolds number the minimum drag coefficients of the small wing are greater than those of the large wing. These differences are believed to be due to a variation of the tunnel-turbulence level with stagnation pressure as was described in connection with the lifts in an earlier section.

For the Reynolds number range of this investigation, the minimum drag coefficients at $M = 1.62$ were found to decrease approximately 29 percent, at $M = 1.94$, 43 percent, and at $M = 2.41$, 38 percent.

Theoretical wave drag coefficients C_{D_w}, laminar skin-friction drags $C_{D_f}(\text{lam})$, and turbulent skin-friction drags $C_{D_f}(\text{turb})$ are also presented in figure 9 as a function of Reynolds number. The theoretical wave-drag coefficients were obtained from reference 10. The Blasius incompressible theory was used to obtain the laminar skin-friction drags whereas the Frankl-Voishel extended theory was used to obtain the turbulent skin-friction drags. The conclusions reached in reference 7 showed that these two skin-friction theories gave satisfactory predictions of experimental skin frictions. A curve representing a summation of C_{D_w} and $C_{D_f}(\text{lam})$ (fig. 9) agrees well with the experimental results (except at the very low Reynolds numbers) at all three Mach numbers up to the point where transition appears to begin. Transition tends to be indicated by the divergence between the experimental results and the theoretical results. As the Reynolds number increases, the minimum drag coefficient of the large wing at $M = 1.62$ increases and approaches the theoretical total drag of the wing having a completely turbulent boundary layer.

CONCLUSIONS

An investigation has been conducted in the Langley 9-inch supersonic tunnel at Mach numbers of 1.62, 1.94, and 2.41 to determine the effects of model scale and stream Reynolds number on the aerodynamic characteristics of two geometrically similar rectangular wings. The wings had symmetrical circular-arc cross sections with aspect ratios of 1.80, thickness ratios of 0.059, and a scale factor of approximately 0.52. The limits of the Reynolds number range for this investigation were 0.13×10^6 and 2.96×10^6. The following conclusions are indicated:

1. Little or no scale effect was found over most of the Reynolds number range at the three test Mach numbers. However, at Mach numbers of 1.62 and 1.94, the lift-curve slopes and minimum drag coefficients of the small wing at the higher Reynolds numbers were slightly greater than those of the large wing. This was believed to be due to a relationship between tunnel-turbulence levels and stagnation pressure.

2. With minor exceptions at the very low Reynolds numbers of these tests, the effect of increasing Reynolds number (by increasing tunnel stagnation pressure) was to increase the lift, decrease the pitching moment, and decrease the drag in a manner consistent with the change in laminar skin-friction drag to a point where transition appeared to occur.

Langley Aeronuatical Laboratory,
National Advisory Committee for Aeronautics,
Langley Field, Va., April 12, 1955.

REFERENCES

1. Quinn, John H., Jr. and Tucker, Warren A.: Scale and Turbulence Effects on the Lift and Drag Characteristics of the NACA 65_3-418, a = 1.0 Airfoil Section. NACA WR L-138, 1944. (Formerly NACA ACR L4H11.)

2. Tucker, Warren A., and Wallace, Arthur R.: Scale-Effect Tests in a Turbulent Tunnel of the NACA 65_3-418, a = 1.0 Airfoil Section with 0.20-Airfoil-Chord Split Flap. NACA WR L-128, 1944. (Formerly NACA ACR L4I22.)

3. Muse, Thomas C.: Some Effects of Reynolds and Mach Numbers on the Lift of an NACA 0012 Rectangular Wing in the NACA 19-Foot Pressure Tunnel. NACA WR L-406, 1943. (Formerly NACA CB 3E29.)

4. Abbott, Ira H., Von Doenhoff, Albert E., and Stivers, Louis S., Jr.: Summary of Airfoil Data. NACA Rep. 824, 1945. (Supersedes NACA WR L-560.)

5. Ferri, Antonio: Completed Tabulation in the United States of Tests of 24 Airfoils at High Mach Numbers (Derived from Interrupted Work at Guidonia, Italy, in the 1.31- by 1.74-Foot High-Speed Tunnel). NACA WR L-143, 1945. (Formerly NACA ACR L5E21, 1945.)

6. Hightower, Ronald C.: Lift, Drag, and Pitching Moment of Low-Aspect-Ratio Wings at Subsonic and Supersonic Speeds - Comparison of Three Wings of Aspect Ratio 2 of Rectangular, Swept-Back, and Triangular Plan Form, Including Effects of Thickness Distribution. NACA RM A52L02, 1953.

7. Love, Eugene S., Coletti, Donald E., and Bromm, August F., Jr.: Investigation of the Variation With Reynolds Number of the Base, Wave, and Skin-Friction Drag of a Parabolic Body of Revolution (NACA RM-10) at Mach Numbers of 1.62, 1.93, and 2.41 in the Langley 9-Inch Supersonic Tunnel. NACA RM L52H21, 1952. (Declassified from Confidential, 10-12-54.)

8. Grigsby, Carl E., and Ogburn, Edmund L.: Investigation of Reynolds Number Effects for a Series of Cone-Cylinder Bodies at Mach Numbers of 1.62, 1.93, and 2.41. NACA RM L53H21, 1953.

9. Jones, Arthur L., Sorenson, Robert M., and Lindler, Elizabeth E.: The Effects of Sideslip, Aspect Ratio, and Mach Number of the Lift and Pitching Moment of Triangular, Trapezoidal, and Related Plan Forms in Supersonic Flow. NACA TN 1916, 1949.

10. Harmon, Sidney M.: Theoretical Supersonic Wave Drag of Untapered Sweptback and Rectangular Wings at Zero Lift. NACA TN 1449, 1947.

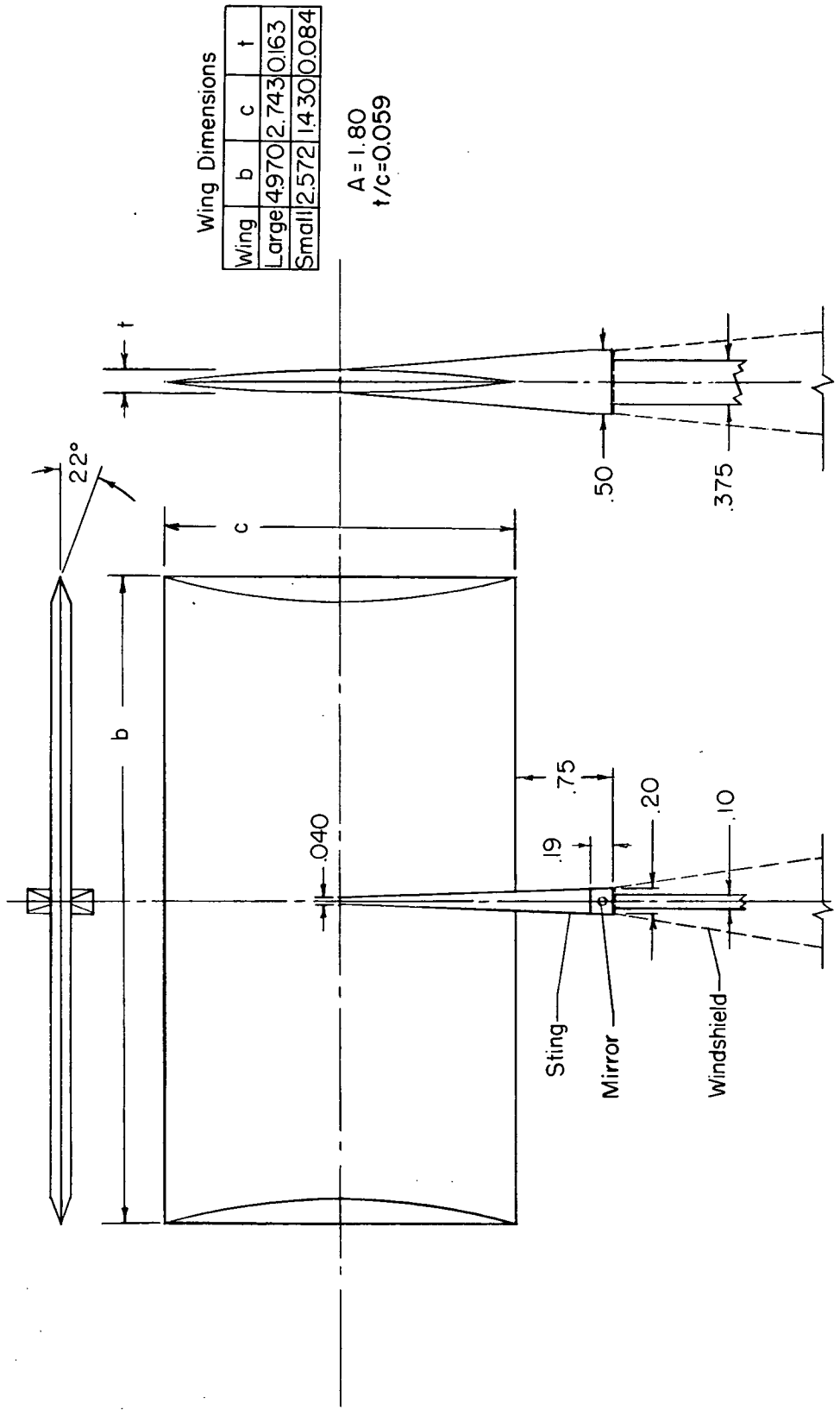

Figure 1.- Sketch of model assembly with the geometric parameters of the two wings. Dimensions on sting and windshield are for large wing. Similar dimensions on small wing are reduced by an average factor of 0.52. All dimensions are in inches.

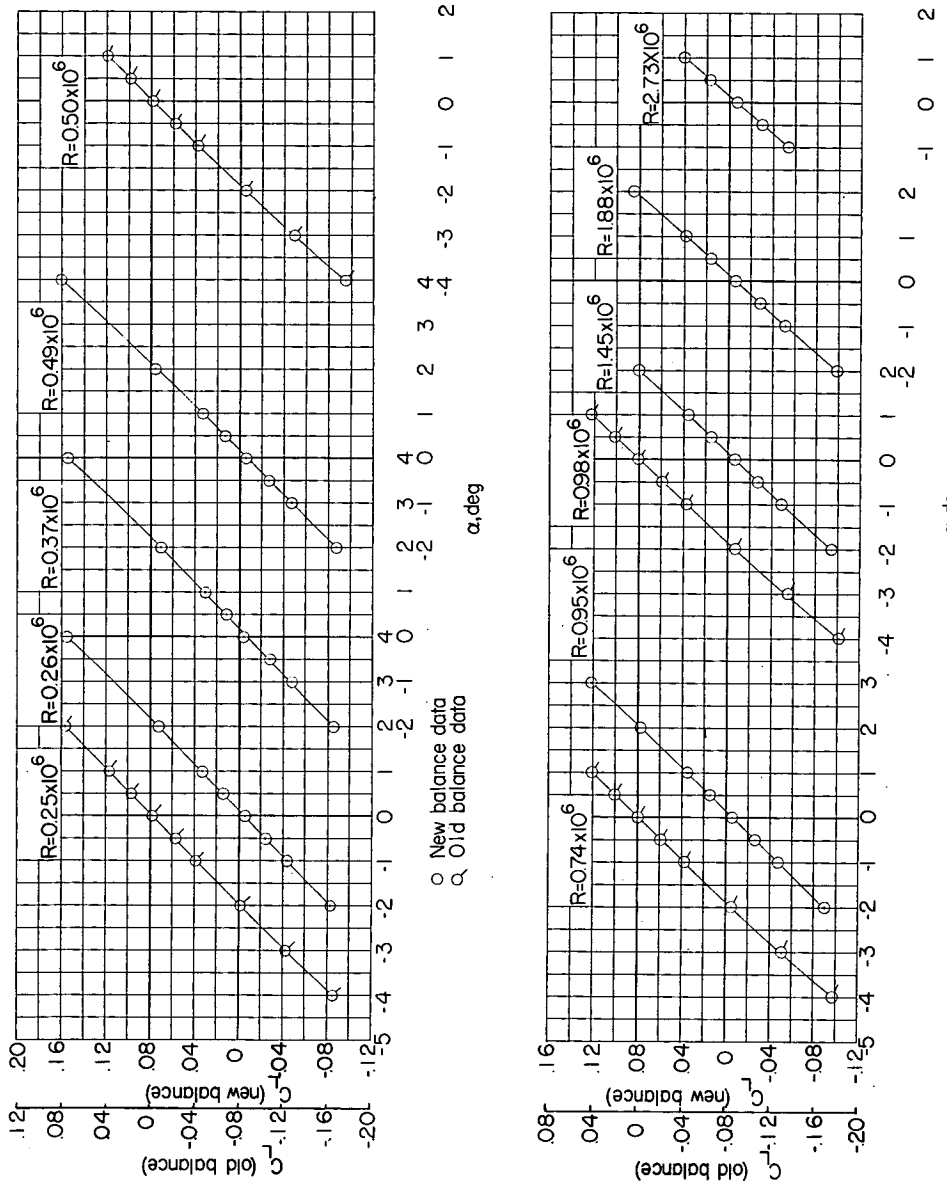

(a) Lift coefficient.

Figure 2.- Aerodynamic characteristics of the large A = 1.80 rectangular wing at M = 1.62 for various Reynolds numbers.

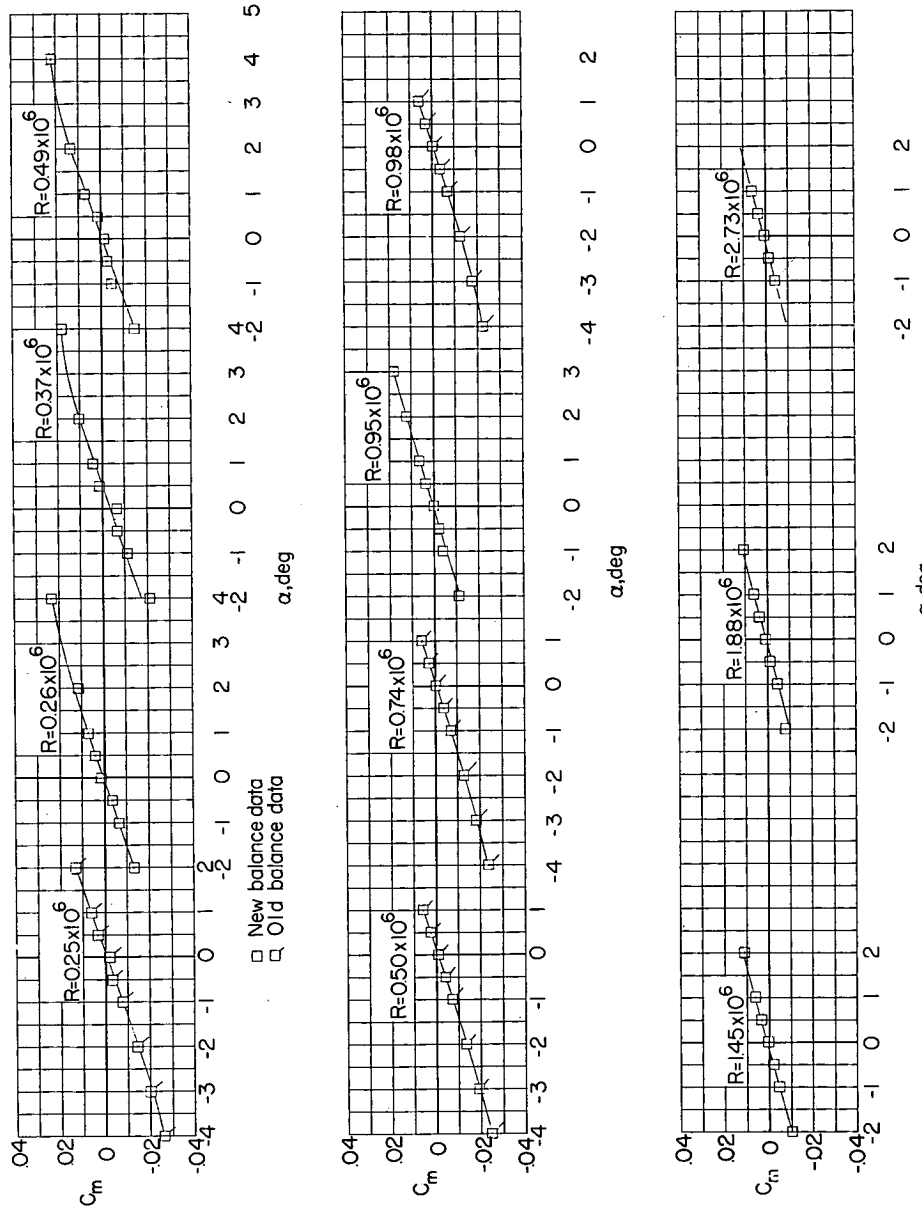

(b) Pitching-moment coefficient.

Figure 2.- Continued.

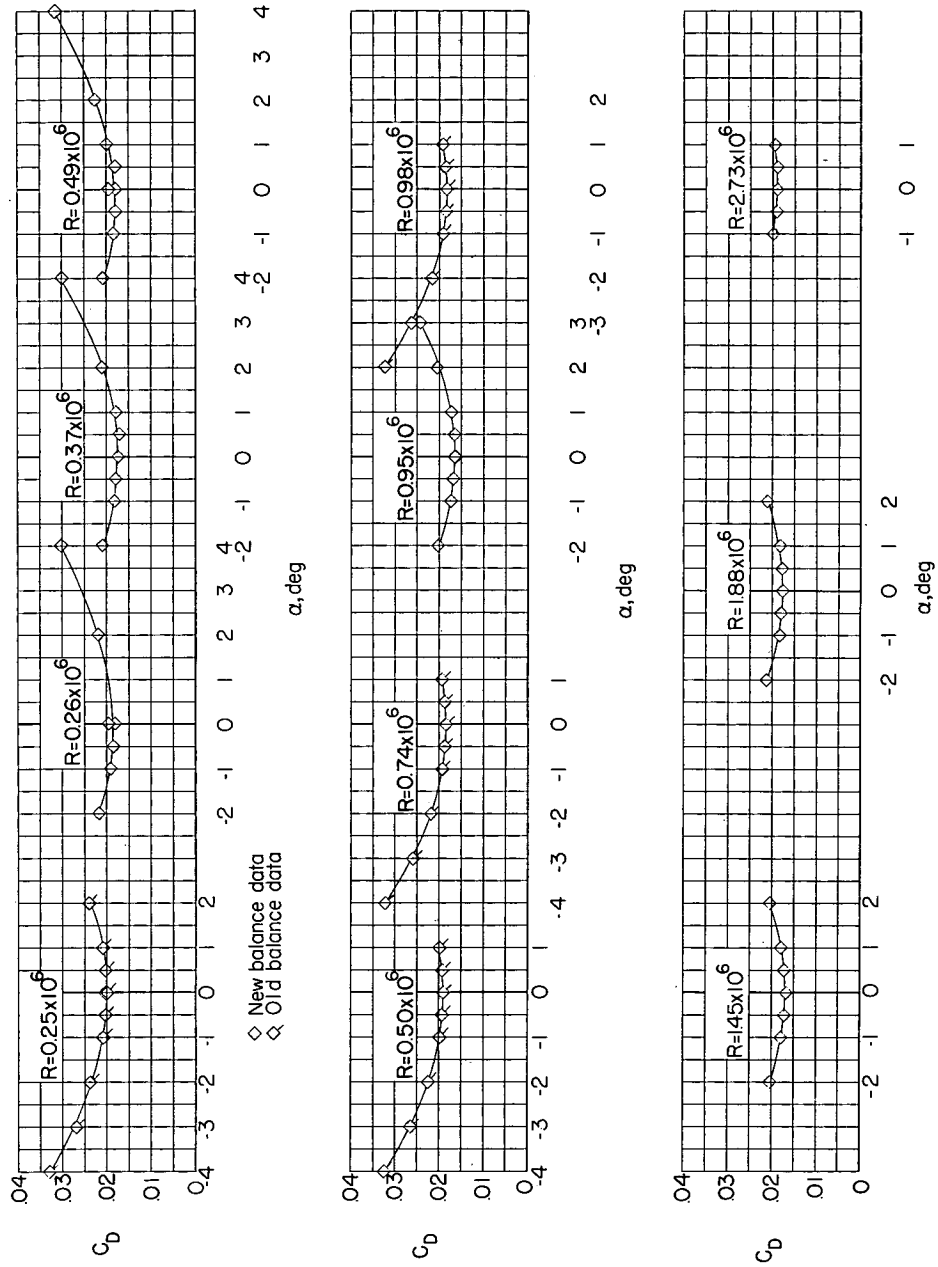

(c) Drag coefficient.

Figure 2.- Concluded.

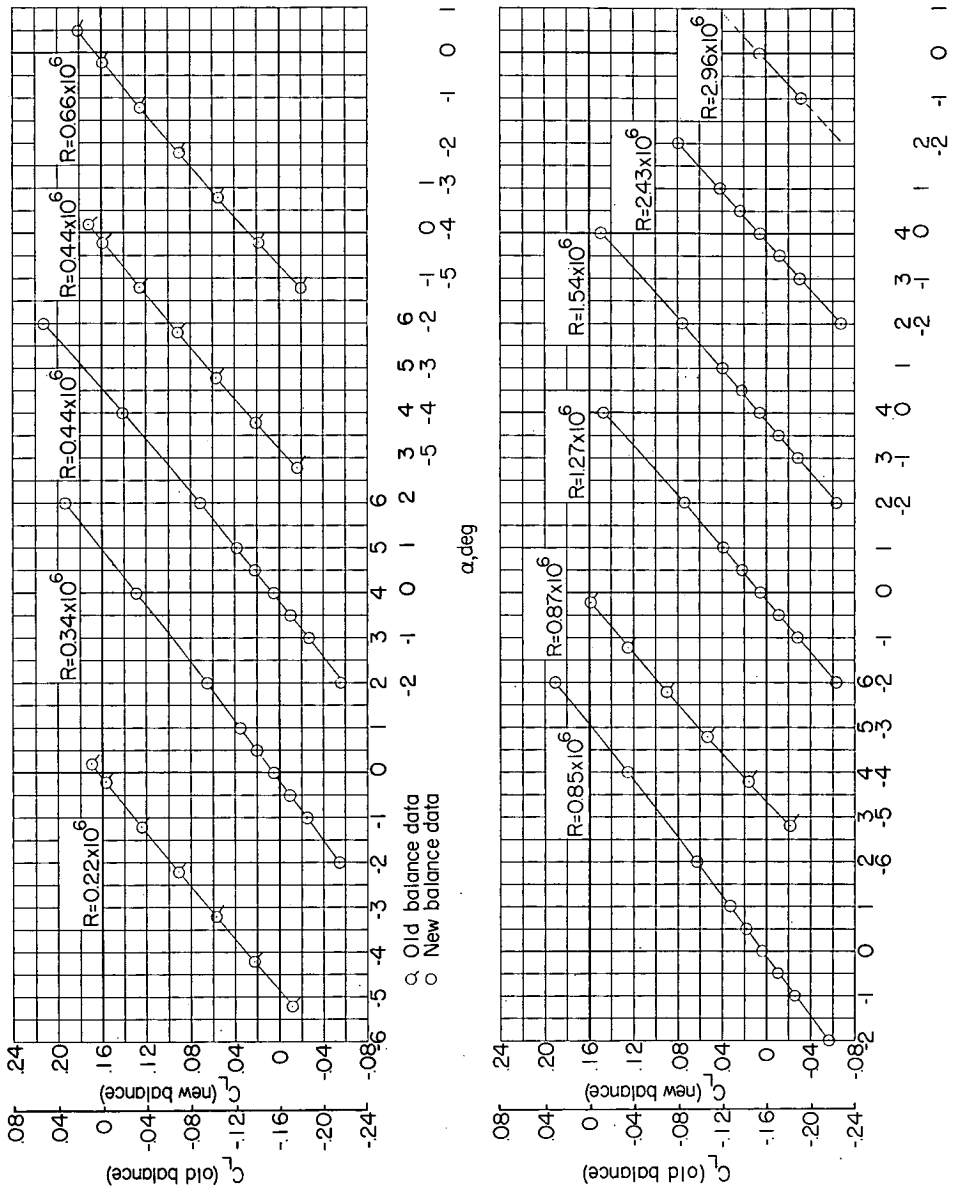

(a) Lift coefficient.

Figure 3.- Aerodynamic characteristics of the large A = 1.80 rectangular wing at M = 1.94 for various Reynolds numbers.

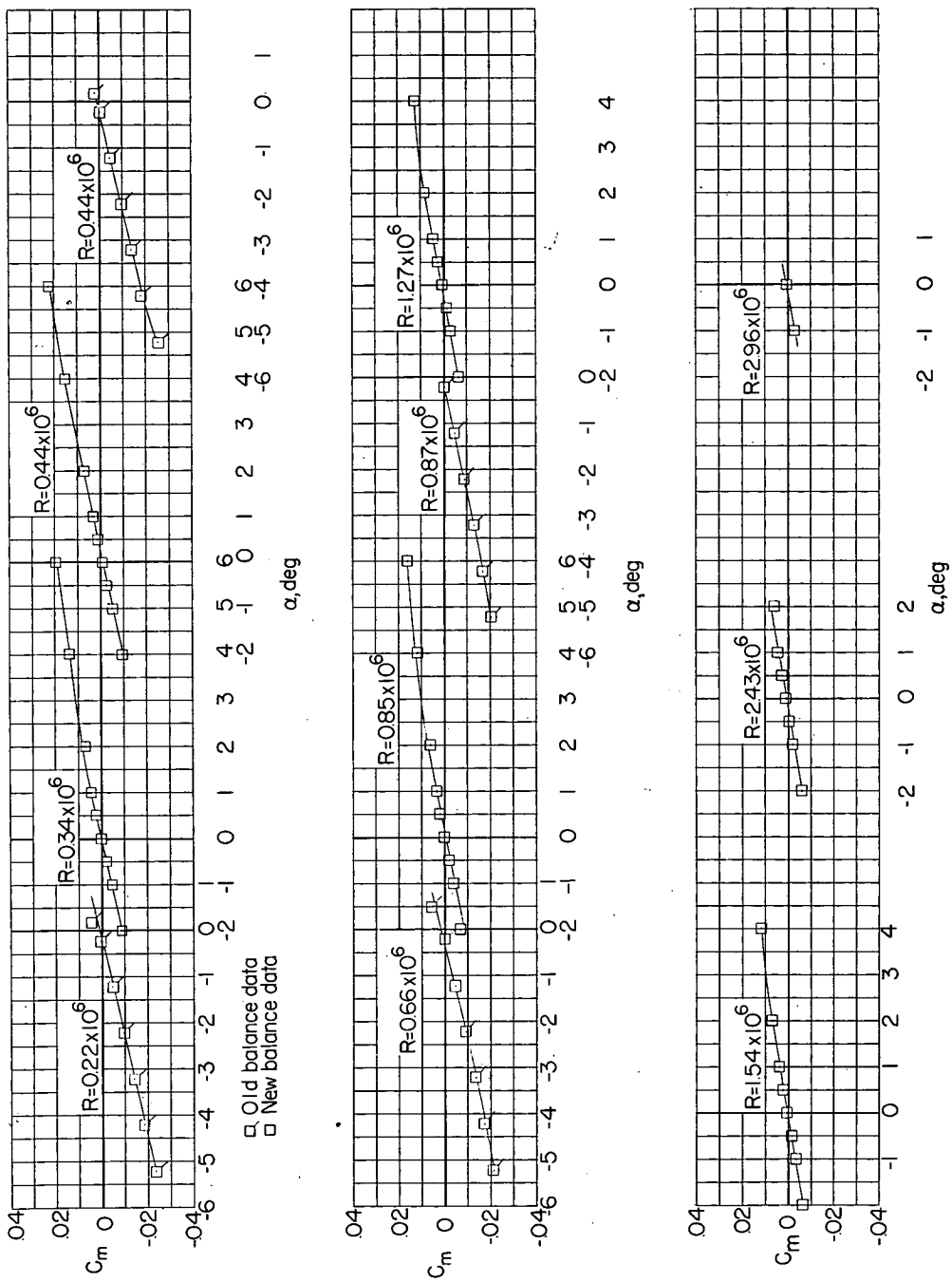

(b) Pitching-moment coefficient.

Figure 3.- Continued.

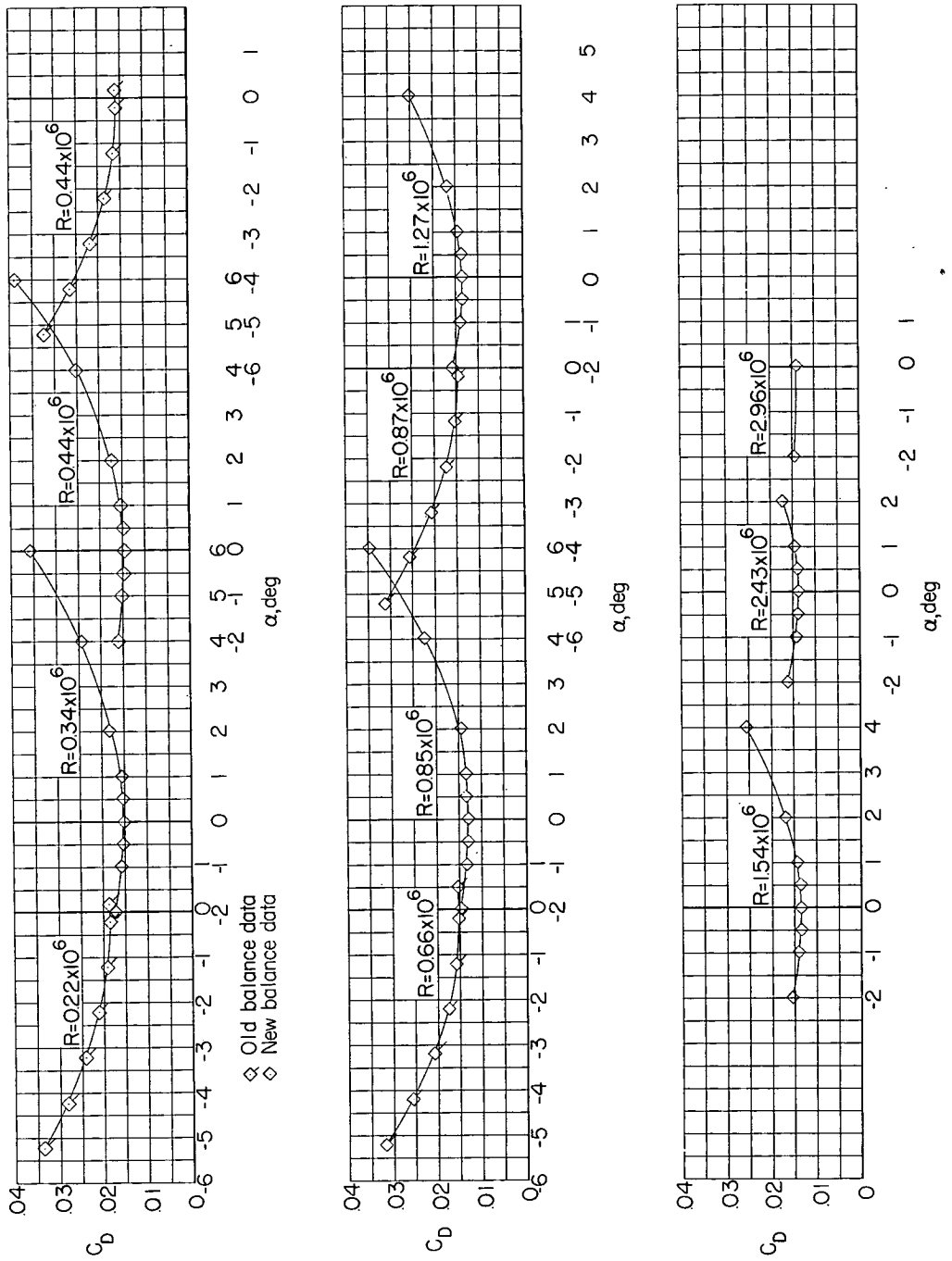

(c) Drag coefficient.

Figure 3.- Concluded.

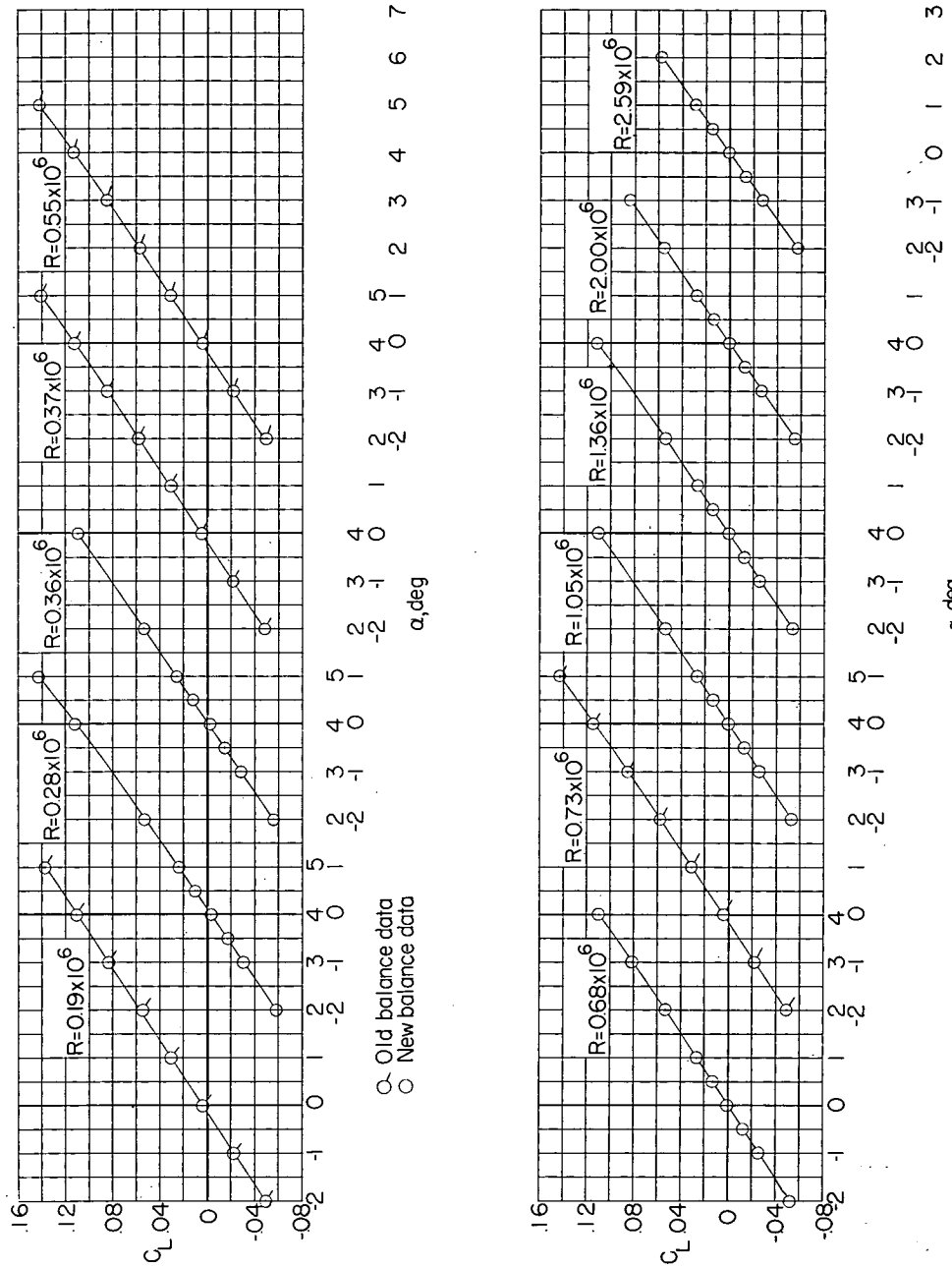

(a) Lift coefficient.

Figure 4.- Aerodynamic characteristics of the large A = 1.80 rectangular wing at M = 2.41 for various Reynolds numbers.

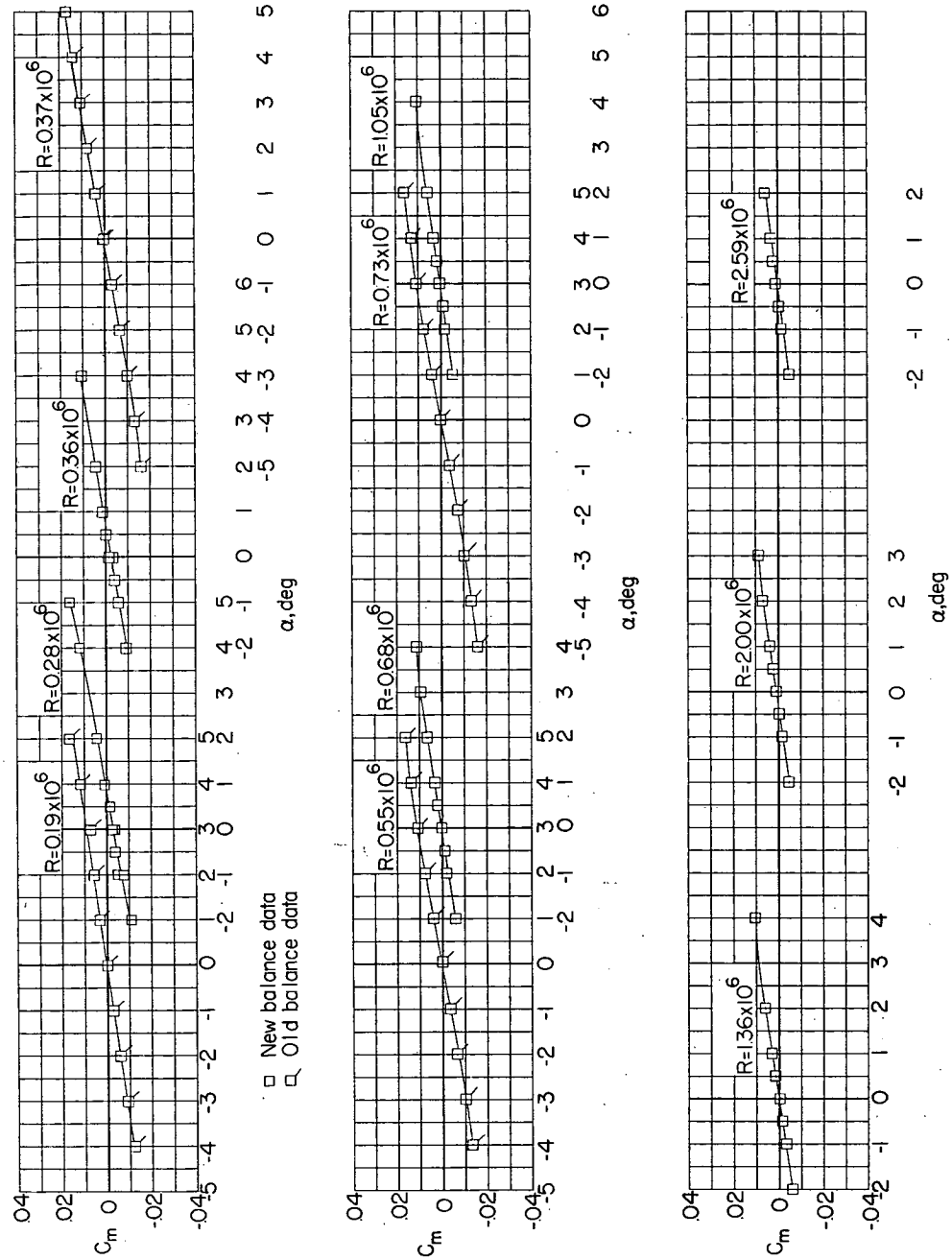

(b) Pitching-moment coefficient.

Figure 4.- Continued.

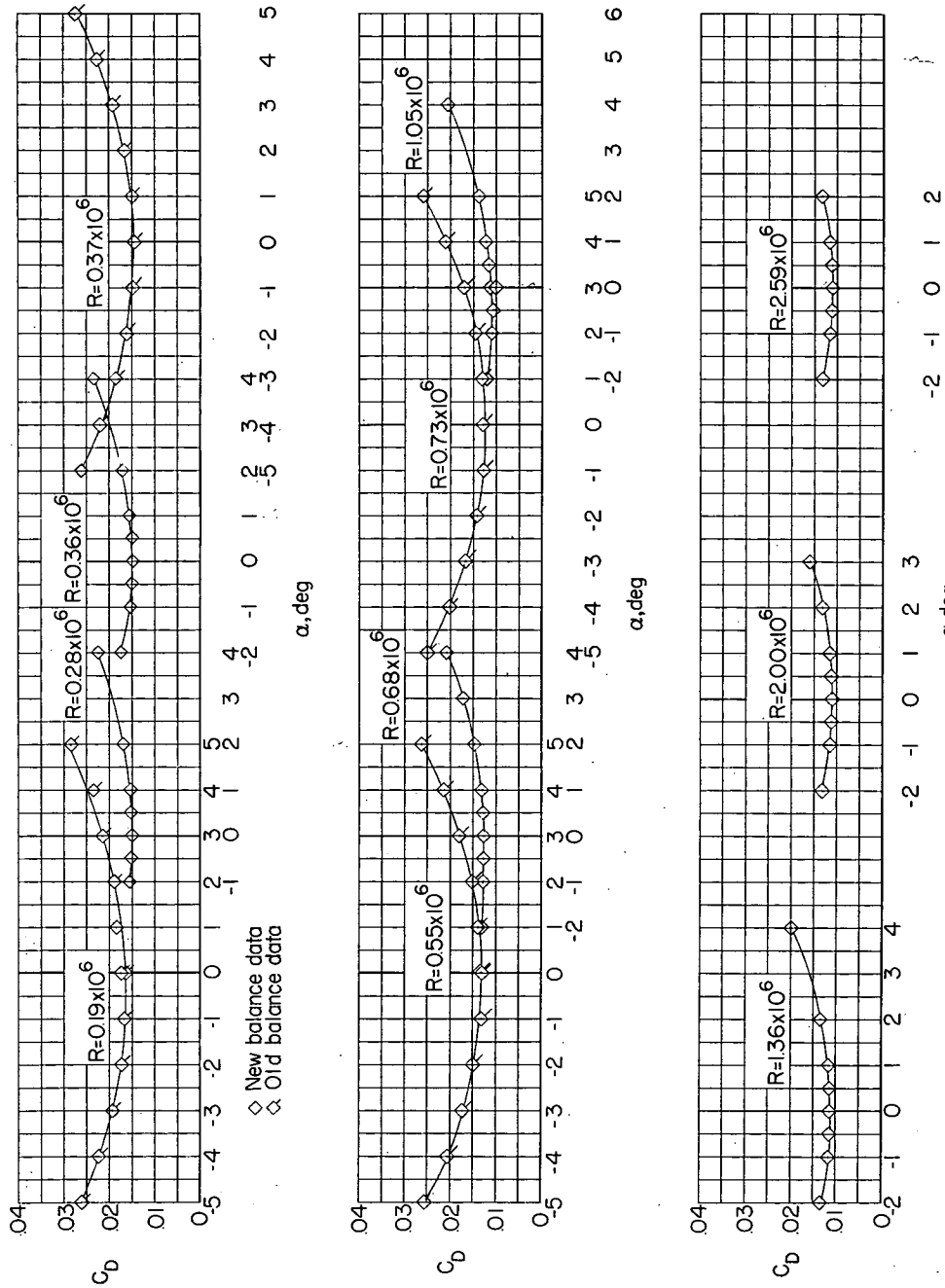

(c) Drag coefficient.

Figure 4.- Concluded.

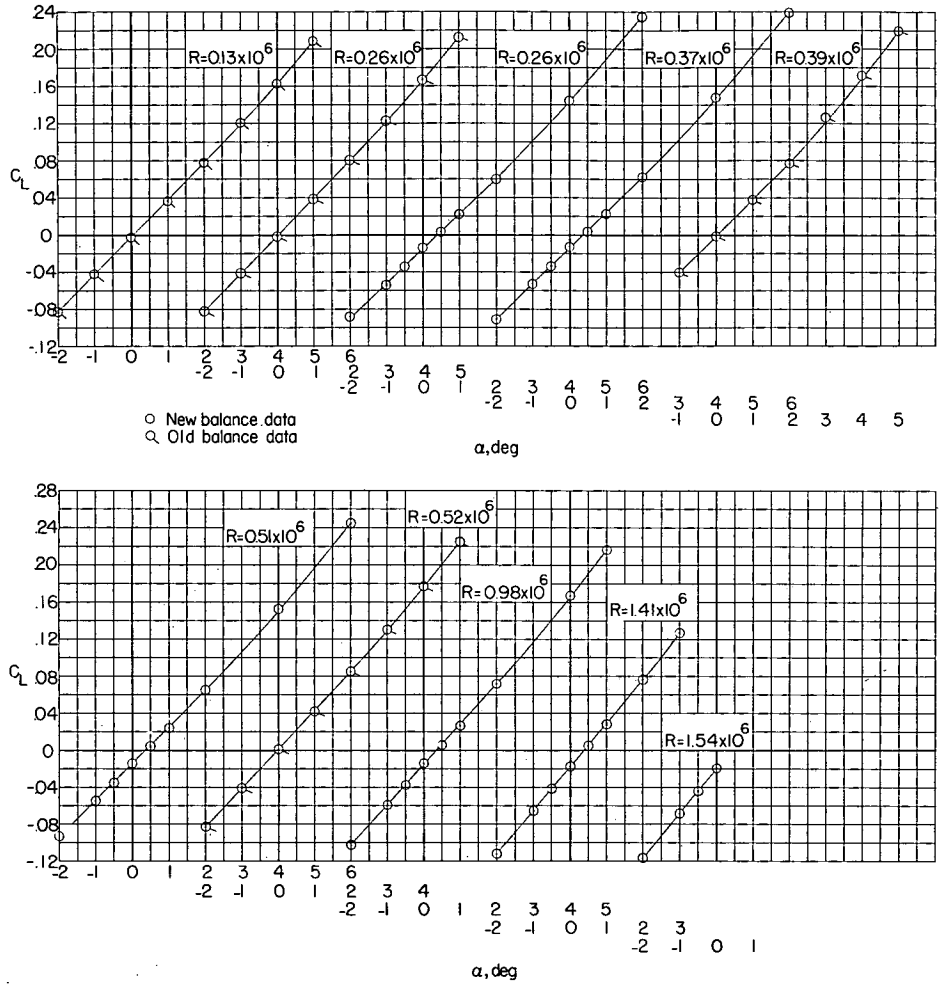

(a) Lift coefficient.

Figure 5.- Aerodynamic characteristics of the small A = 1.80 rectangular wing at M = 1.62 for various Reynolds numbers.

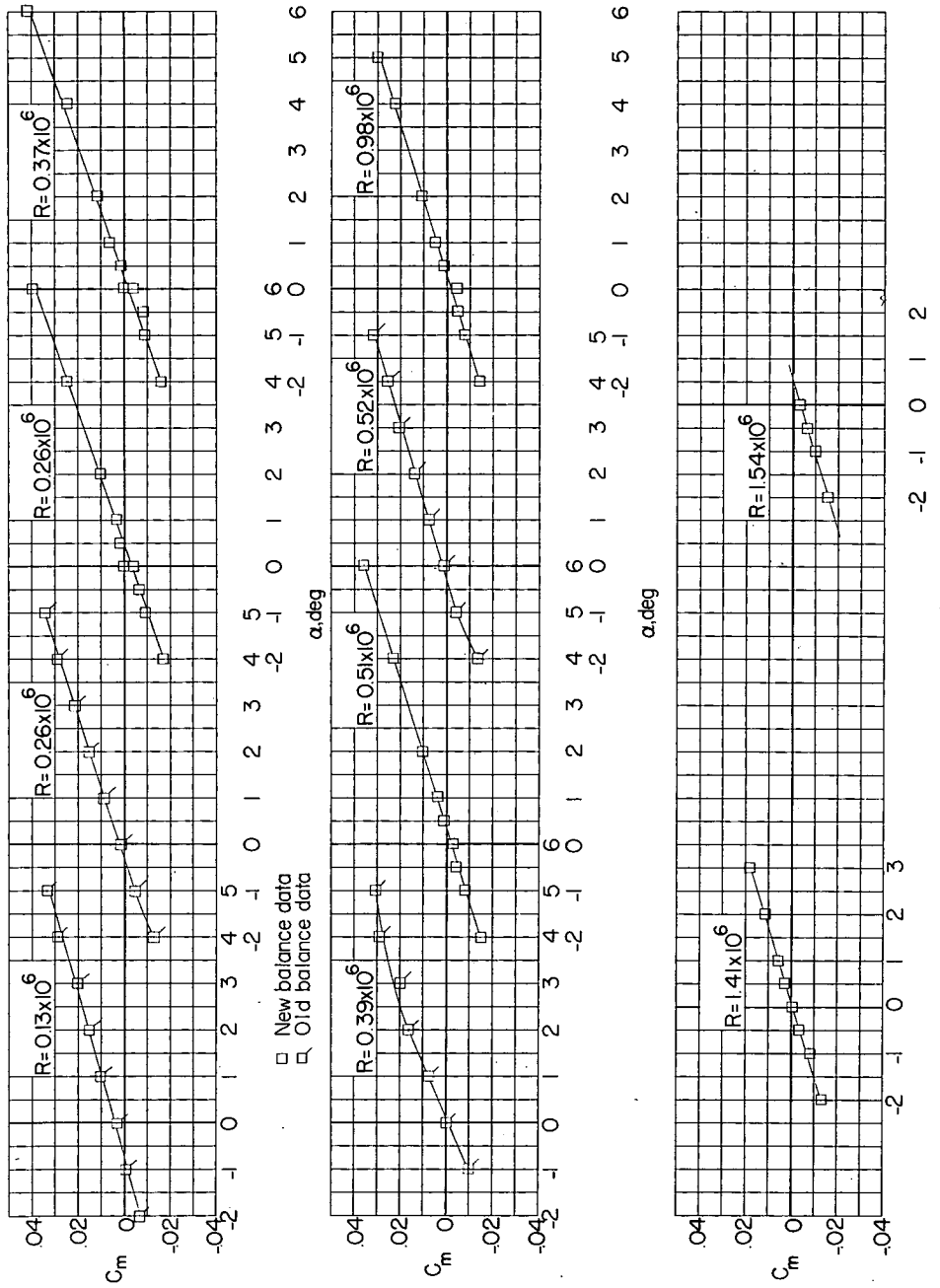

(b) Pitching-moment coefficient.

Figure 5.- Continued.

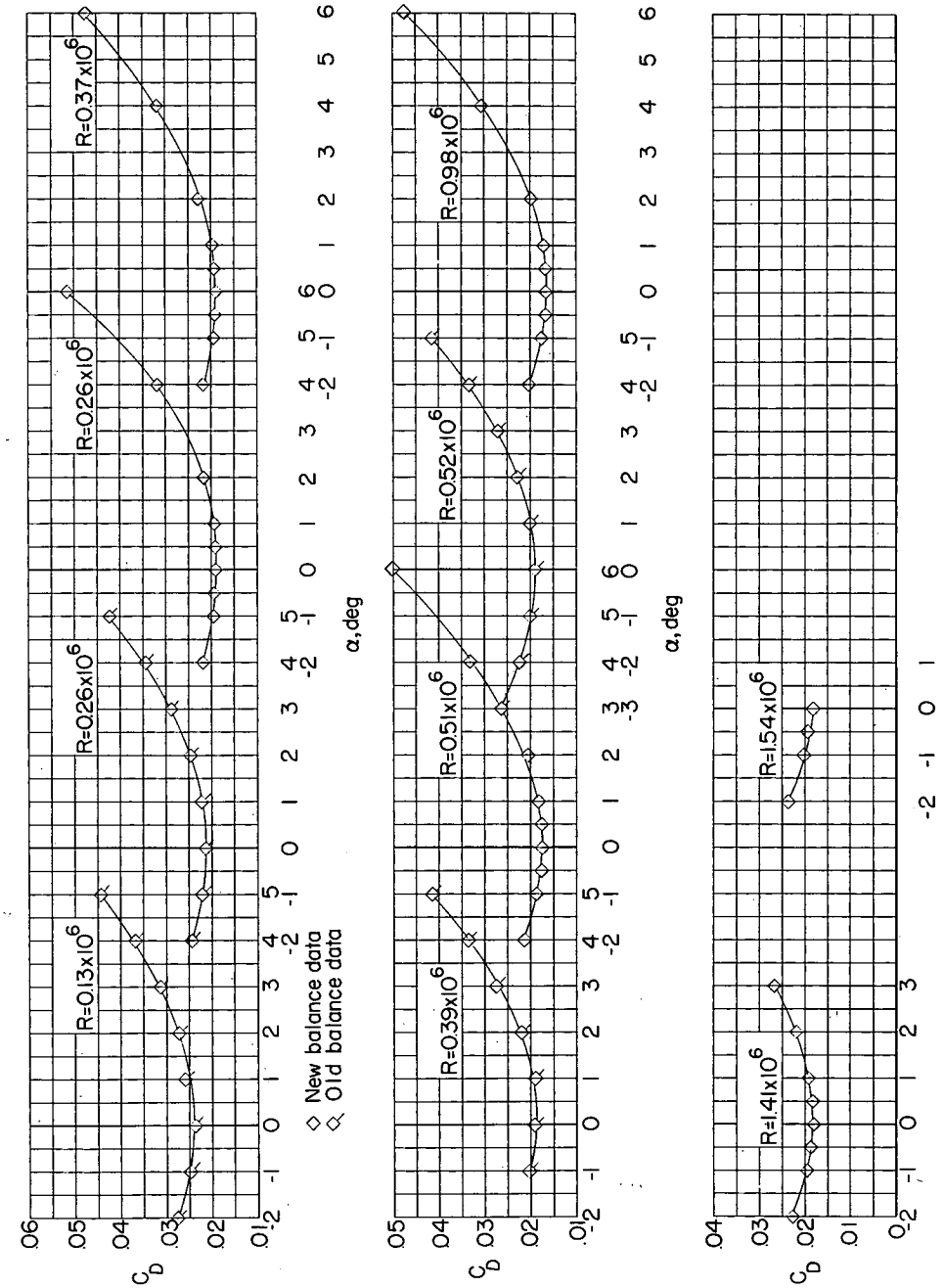

(c) Drag coefficient.

Figure 5.- Concluded.

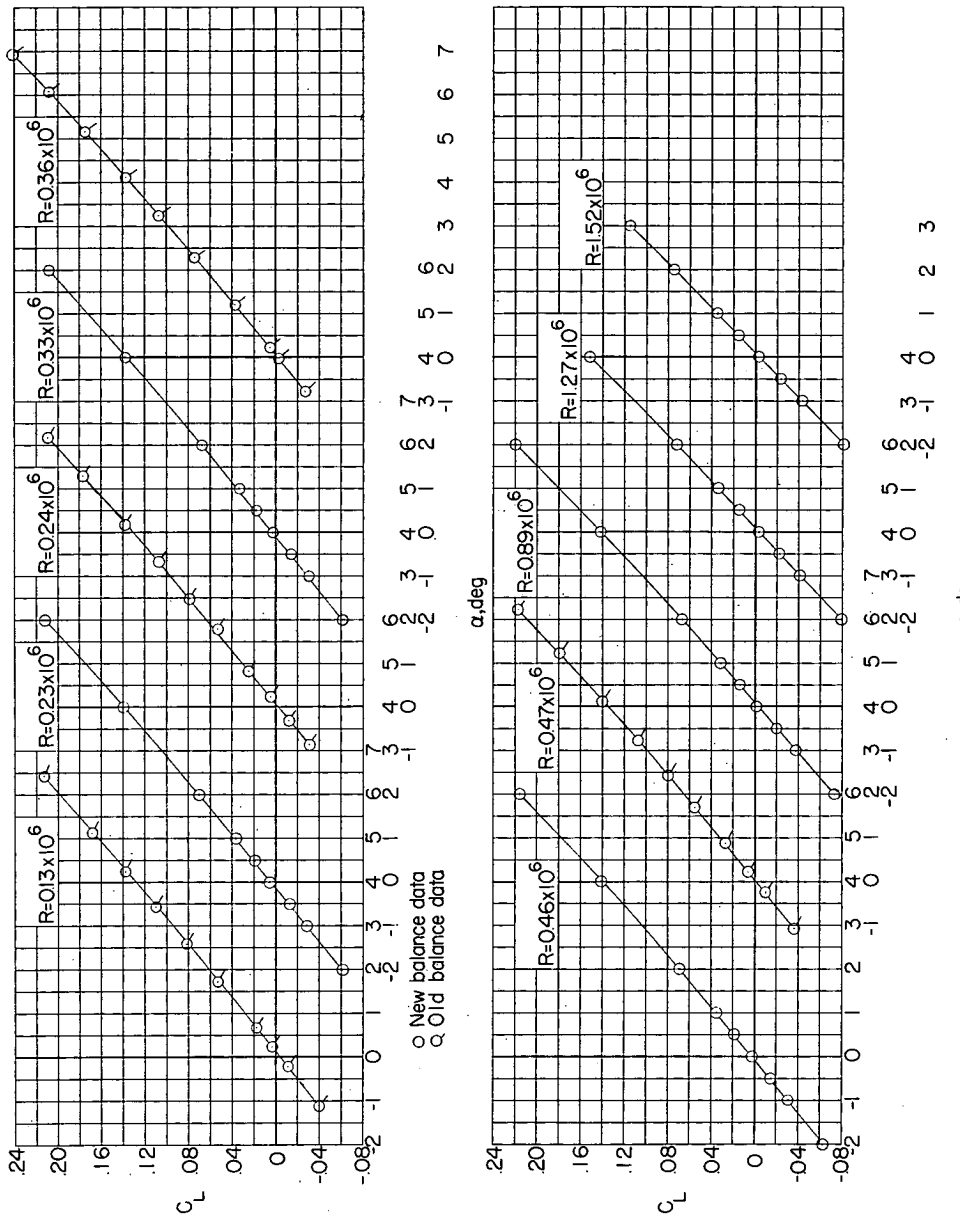

(a) Lift coefficient.

Figure 6.- Aerodynamic characteristics of the small A = 1.80 rectangular wing at M = 1.94 for various Reynolds numbers.

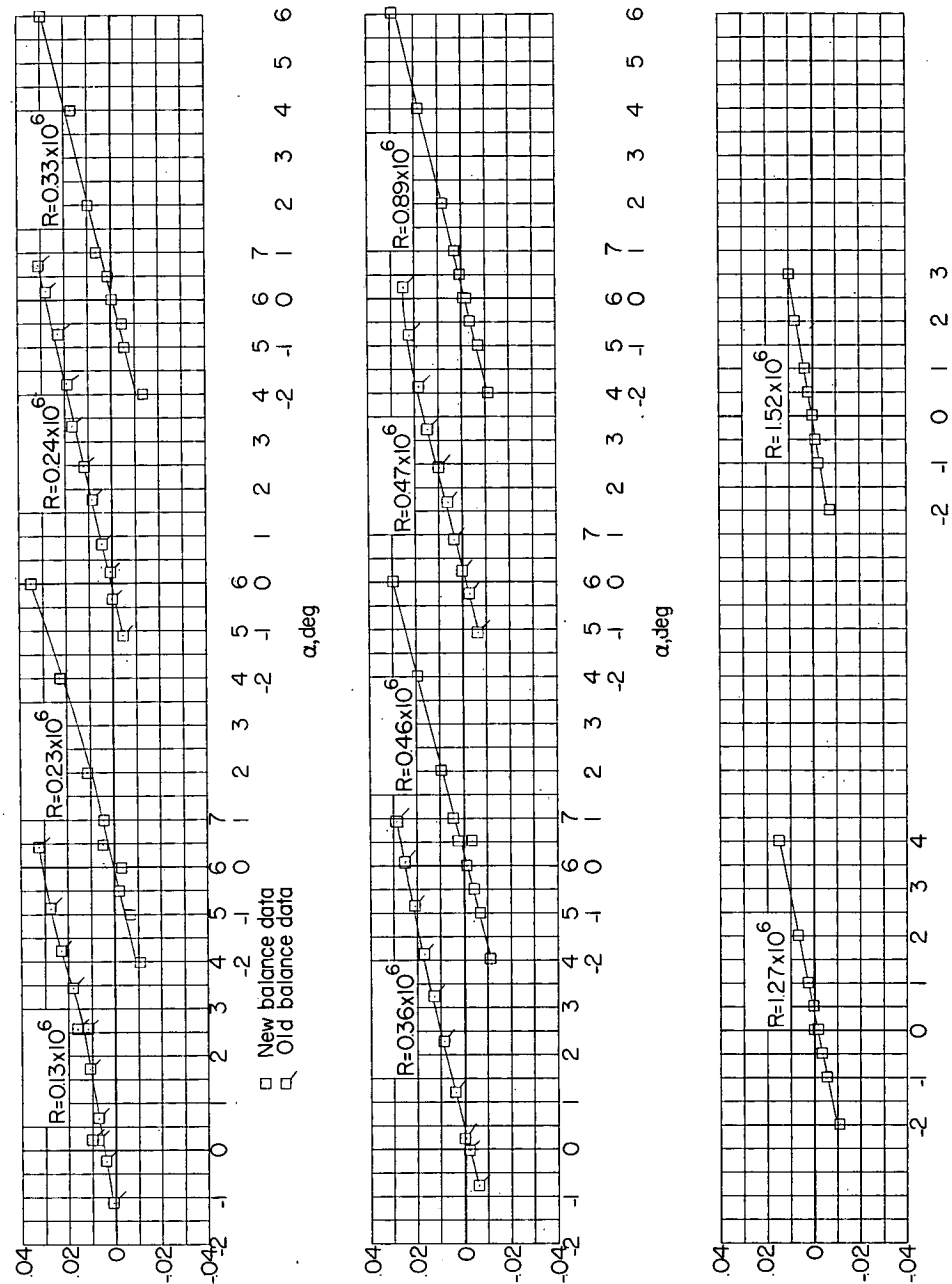

(b) Pitching-moment coefficient.

Figure 6.- Continued.

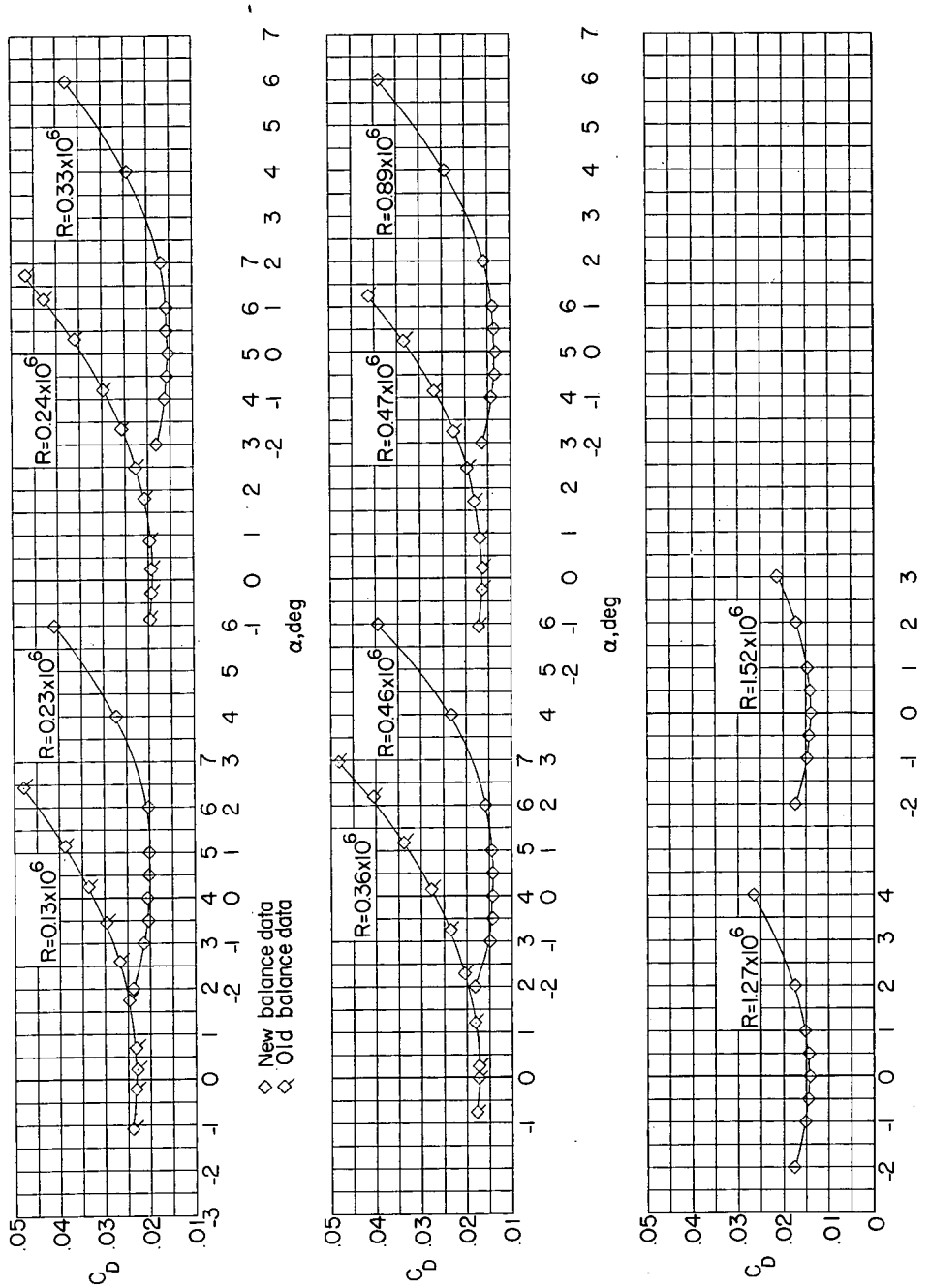

(c) Drag coefficient.

Figure 6.- Concluded.

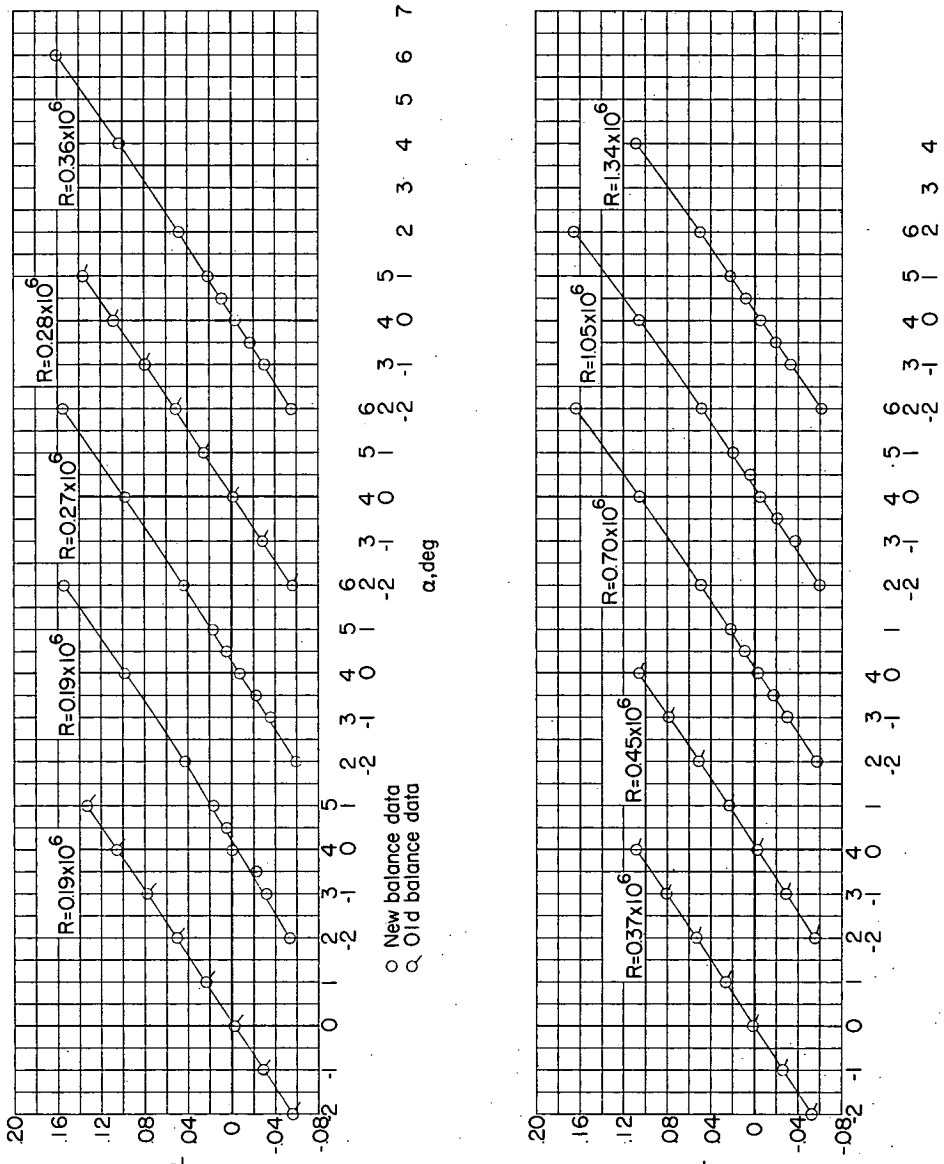

(a) Lift coefficient.

Figure 7.- Aerodynamic characteristics of the small A = 1.80 rectangular wing at M = 2.41 for various Reynolds numbers.

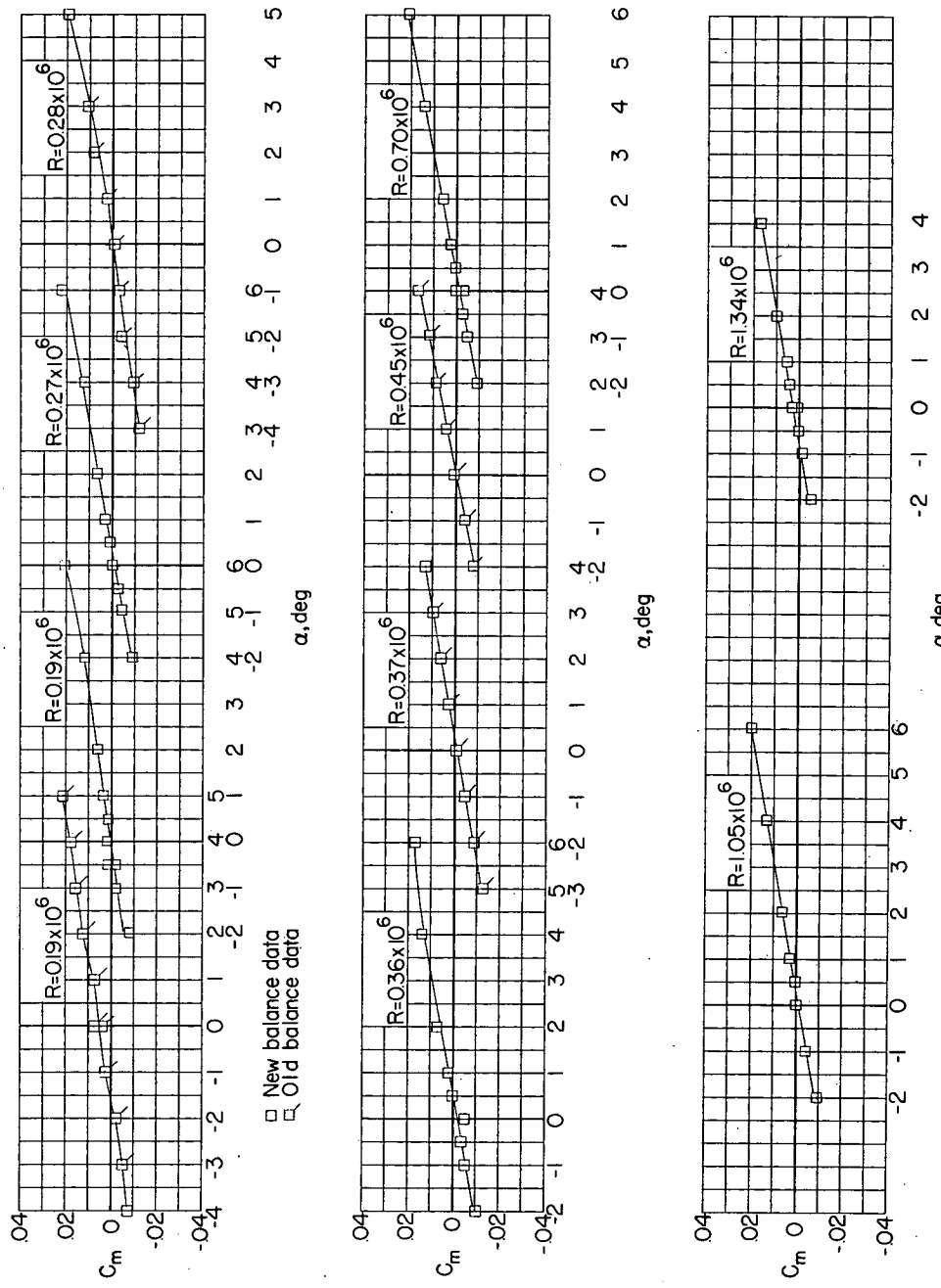

(b) Pitching-moment coefficient.

Figure 7.- Continued.

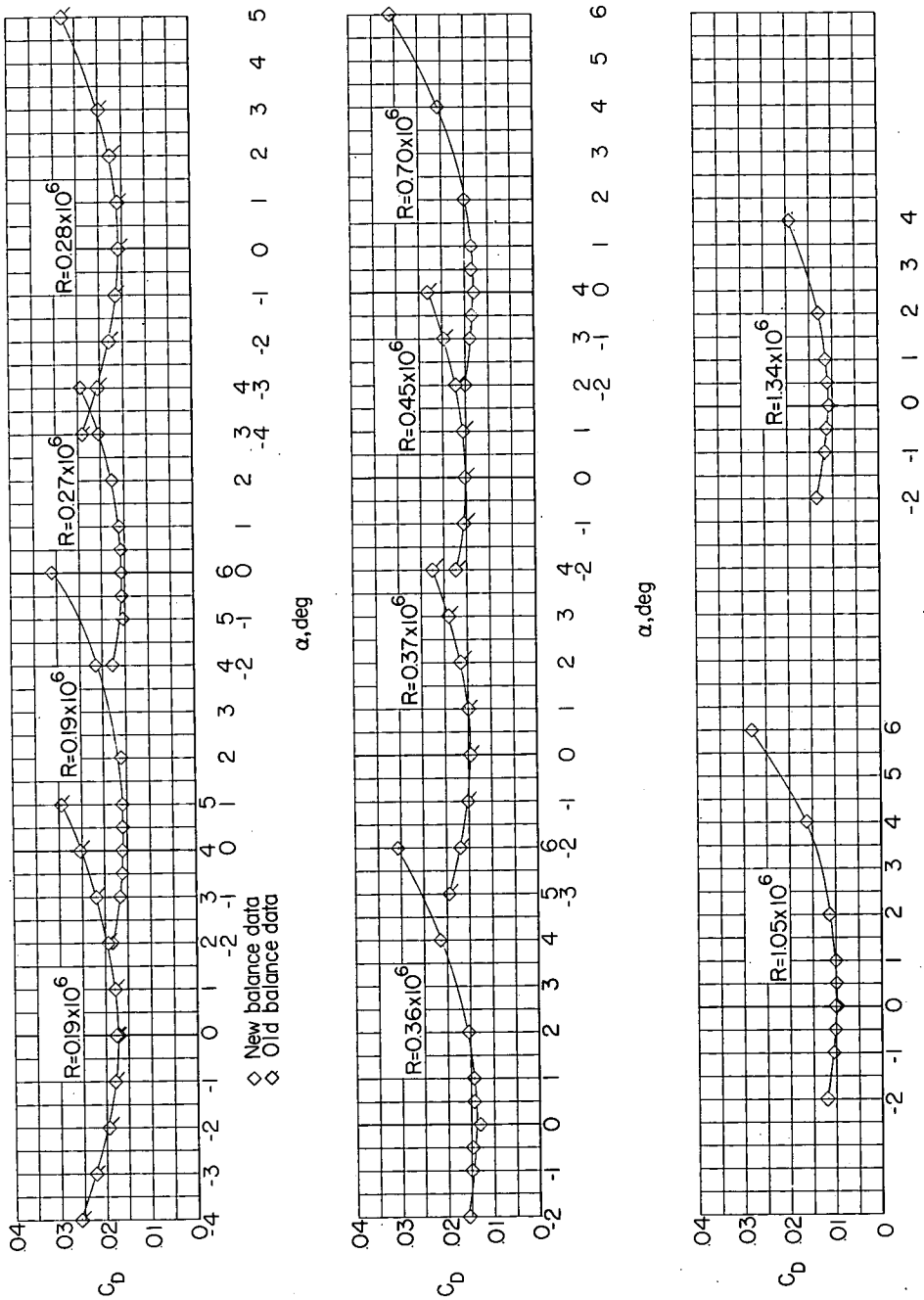

(c) Drag coefficient.

Figure 7.- Concluded.

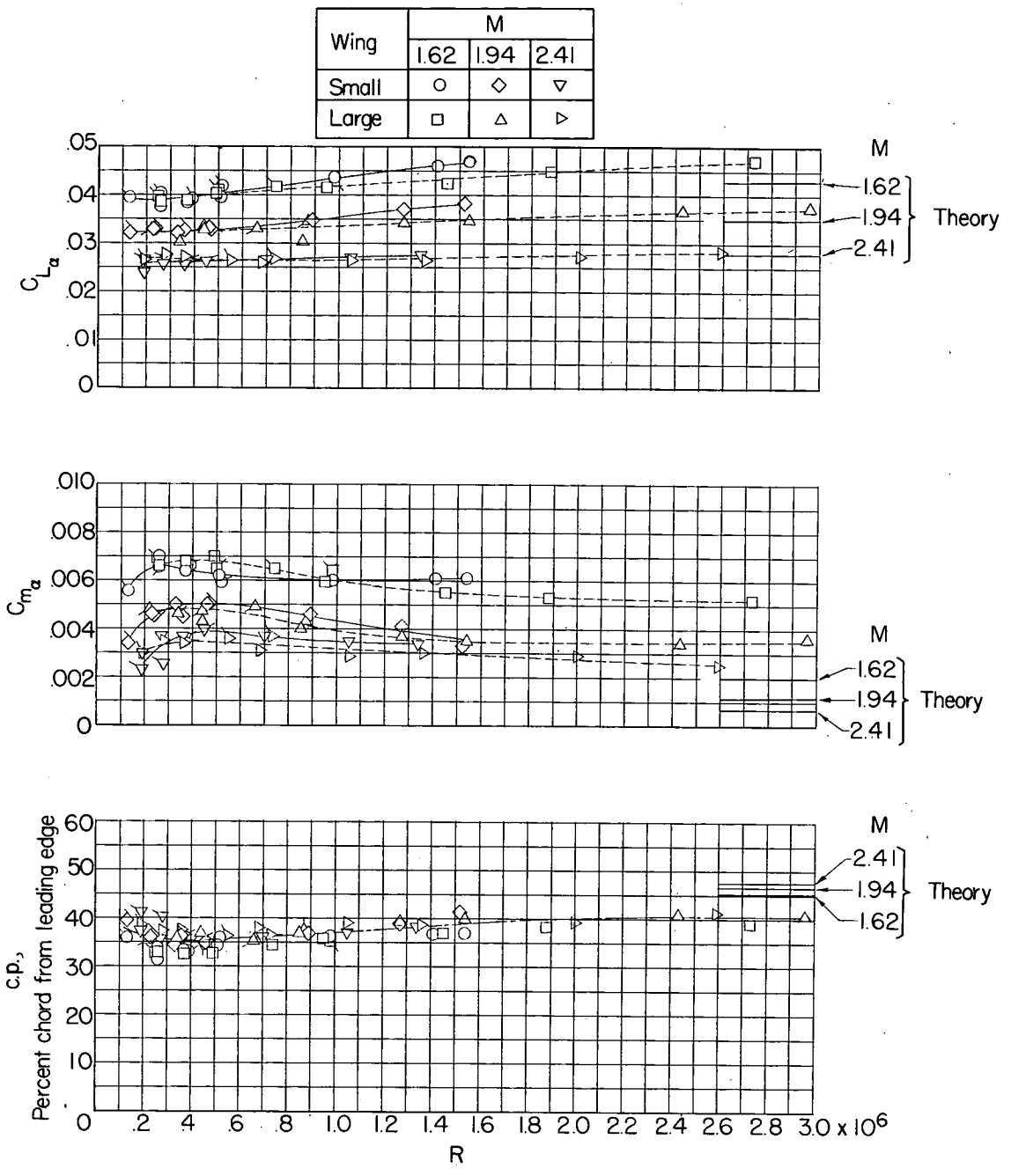

Figure 8.- Variation of the lift-curve slopes, pitching-moment-curve slopes, and center-of-pressure location of the two A = 1.80 rectangular wings with Reynolds number at M = 1.62, 1.94, and 2.41. Flagged symbols denote old-balance data.

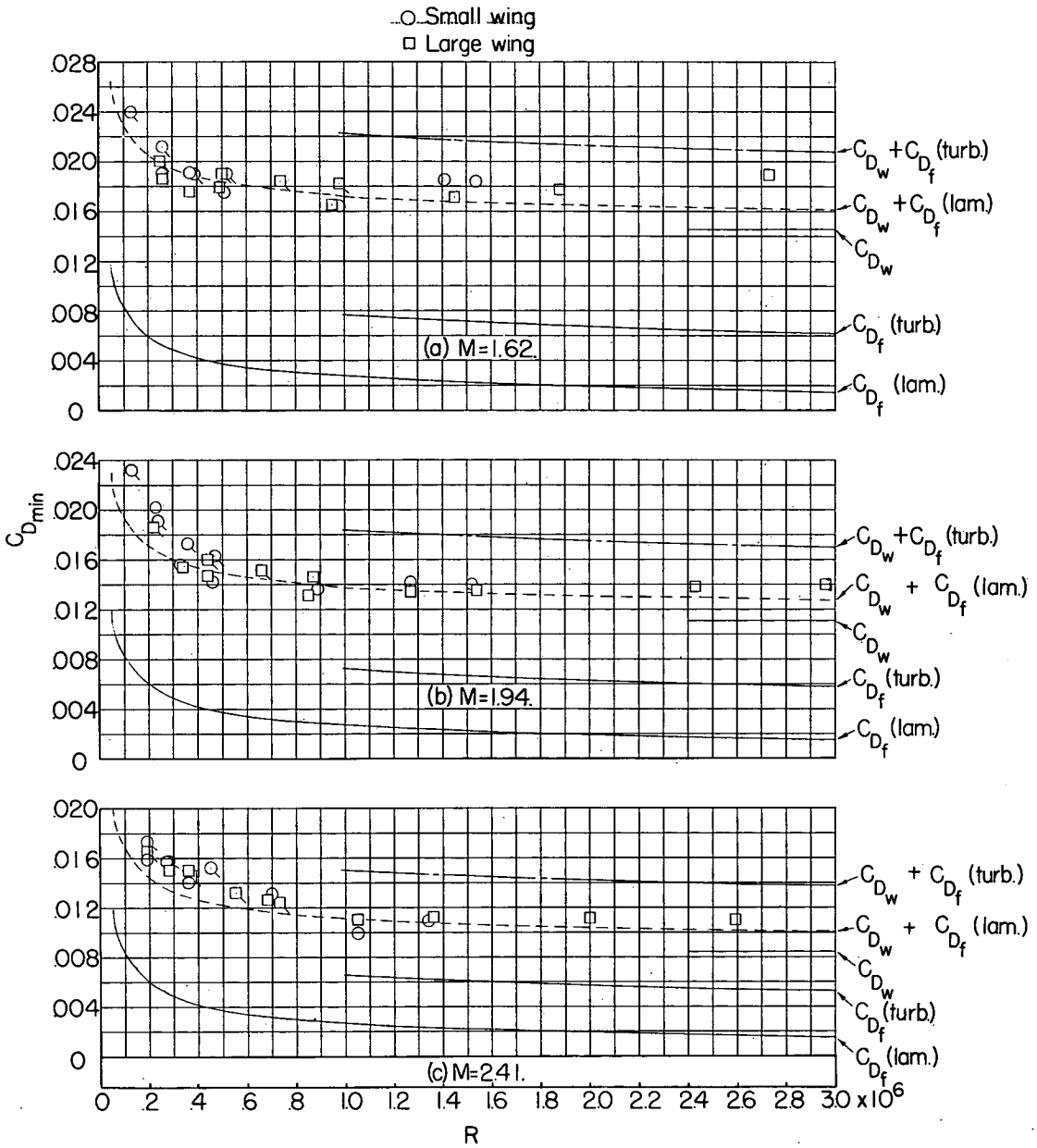

Figure 9.- Variation of the minimum drag values of the two A = 1.80 rectangular wings with Reynolds number at M = 1.62, 1.94, and 2.41. Flagged symbols denote old-balance data.